



UvA-DARE (Digital Academic Repository)

Materials and devices for spatial multi-dimensional liquid chromatography

Passamonti, M.

Publication date
2022

[Link to publication](#)

Citation for published version (APA):

Passamonti, M. (2022). *Materials and devices for spatial multi-dimensional liquid chromatography*. [Thesis, fully internal, Universiteit van Amsterdam].

General rights

It is not permitted to download or to forward/distribute the text or part of it without the consent of the author(s) and/or copyright holder(s), other than for strictly personal, individual use, unless the work is under an open content license (like Creative Commons).

Disclaimer/Complaints regulations

If you believe that digital publication of certain material infringes any of your rights or (privacy) interests, please let the Library know, stating your reasons. In case of a legitimate complaint, the Library will make the material inaccessible and/or remove it from the website. Please Ask the Library: <https://uba.uva.nl/en/contact>, or a letter to: Library of the University of Amsterdam, Secretariat, P.O. Box 19185, 1000 GD Amsterdam, The Netherlands. You will be contacted as soon as possible.

Chapter 5

3D-printed microfluidic devices for spatial multi-dimensional liquid chromatography

Abstract

In this study, we designed and 3D-printed several microfluidic devices suitable for multi-dimensional spatial liquid-chromatography separations. Three approaches to achieve flow confinement were evaluated, based on previous works. In the device called “channel of separation with many individual controls” (COSMIC), a cold fluid circulates inside a jacket around the first-dimension (¹D) channel in order to create frozen plugs in the outlets. This led to successful confinement of the ¹D flow under certain conditions. The “two-dimensional insertable separation tool” (TWIST) consists of a channel with through-holes that can be aligned and misaligned inside a second-dimension (²D) part with corresponding through-holes. Inadequate flow confinement in the TWIST led to the design of an improved “simple-liquid-transfer” (SLIT) tool with good success, with some restrictions on the materials available. Finally, an extended version of the COSMIC device was constructed, that incorporated ²D channels. In this device, we attempted to achieve flow confinement by creating higher permeabilities in the ¹D domain as compared to the ²D domain. Based on the success of the COSMIC approach, the ¹D channel was packed with C18-modified silica particles and used for the separation of a mixture of small molecules.

5.1 Introduction

The demand for separation power comes from many fields, such as food, life and environmental science. For example, in proteomics, analytical chemists are confronted with the need to separate and characterize complex mixtures with tens of thousands of analytes in the shortest possible time¹. Conventional one-dimensional liquid-chromatography (1D-LC) systems cannot provide the needed separation power and this is why comprehensive two-dimensional liquid chromatography (LC×LC) has emerged in the last 20 years². Typically, in column-based, “temporal” LC×LC separations, sample and solvents are flushed through the columns. Fractions of the effluent of the first-dimension (¹D) column are transferred to the second-dimension (²D) column for further separation, with the aid of a modulator. However, temporal LC×LC methods are still challenging and time-consuming to develop and to perform. An alternative approach is to perform spatial multi-dimensional liquid chromatography. In spatial separations, the sample and the solvents move across the separation bed and the analytes get separated within one bed volume, with the most retained compound moving the least. After the first-dimension separation, in spatial 2D-LC, fractions are transferred all at the same time to the second dimension for further separation, through the use of a flow distributor (FD). The potential of spatial multi-dimensional LC has been described in detail by Wouters *et al.*³ In their paper, flow confinement is identified as one of the major challenges. Any spillage from the first dimension will lead to losses in separation performance.

For the separation of peptides in a chip, Liu *et al.*⁴ used geometrical constrictions to achieve flow confinement between dimensions in a device that combined iso-electric focusing (IEF) with LC. In 2015 Wouters *et al.*⁵ designed, created and tested a planar microfluidic device to perform spatial 2D-LC. They introduced physical barriers to reduce leakage into the second dimension during the first-dimension separation.

Several options to confine the flow have been studied in recent years. Adamopoulou *et al.*⁶ proposed a modular cylindrical and rotatable device, the TWIST (two-dimensional insertable separation tool). The device comprises a channel with through-holes that can be inserted inside a second-dimension device with corresponding through-holes. The spatial 1D-LC separation takes place when the holes are not aligned, while the fractions can be flushed to the second dimension when the holes are aligned, and the devices are in a flow-through position.

Nawada *et al.*⁷ suggested a freeze-thaw-valve (FTV) approach. The separation channel is enveloped by cooling and heating jackets and a heat-transfer liquid is circulated through the two jackets. Regions of the device can be cooled down to create a frozen barrier that allows the spatial 1D-LC to take place in a confined channel and subsequently, heated up to transfer the fractions to the second dimension. A channel of separation with many individual controls (COSMIC) was designed with 33 FTVs to prove the scalability of the approach.

Finally, Adamopoulou *et al.*⁸ suggested the use of different permeabilities across the different compartments of the microfluidic device to achieve flow confinement. Based on computational fluid dynamics (CFD) on spatial 3D-LC devices, it can be concluded that the (¹D) stationary phase must have a permeability that is three orders of magnitude higher than the ²D stationary phase to reach full confinement and avoid spillage.

In this work, we aim to design, create and test 3D-printed titanium devices to confine flow and, eventually, perform spatial 2D-LC separations. To this end, we implemented and tested the FTV approach in the COSMIC device. Subsequently, we updated the design of the COSMIC device, so as to introduce a second-dimension separation body, applying different permeabilities in the different compartments. Finally, as an alternative path to reach our goals, we tested the TWIST approach and adapted this from a circular to a rectangular format (simple liquid transfer, SLIT).

5.2 Experimental section

5.2.1 Materials and methods

Styrene (STY, > 99.5%), divinylbenzene (DVB, 80%), 3-(trimethoxysilyl)propyl methacrylate (γ -MAPS, 98%), 2,2'-azobisisobutyronitrile (AIBN, 98%), *n*-decanol (99%), sodium hydroxide (NaOH), aluminium oxide (Al_2O_3), acrylamide (AA, electrophoresis grade, 99%), N,N'-methylenebisacrylamide (MBA, 99%), 1-octanol (OctOH, 99%), dimethyl sulfoxide (DMSO, >99.9%), dimethylformamide (DMF), thiourea (Thio), uracil (Ura), acetophenone (AP), benzamide, benzyl alcohol, benzonitrile, phenol and pyridine were purchased from Sigma Aldrich (St. Louis, MO, USA). Toluene (Tol), ethanol (EtOH), methanol (MeOH), acetonitrile (ACN) and tetrahydrofuran (THF, >99.8), were purchased from Biosolve (Valkenswaard, The Netherlands). Hydrochloric acid 37% (HCl) was obtained from Acros (Geel, Belgium). Purified water (18.2 M Ω cm) was produced by a Sartorius Arium 611UV Ultrapure Water System (Göttingen, Germany). The titanium devices were designed by us and ordered from Materialise (Leuven, Belgium). The glass-lined tubing (100 mm length, 0.8 mm ID) and the stainless-steel (SS) tubing (200 mm length \times 1 mm ID) were purchased from VICI (Houston, TX, USA).

5.2.2 Device design and 3D-printing

The COSMIC and TWIST devices were previously described by Nawada *et al.*⁷ and by Adamopoulou *et al.*⁶, respectively. Below a short description and pictures of the devices are provided, which are necessary for the discussion in the present paper.

The COSMIC device (Figure 1) was designed with a jacket enveloping the horizontal 1D channel (173 mm \times 1 mm). This channel is connected to 16 T-junctions above and 17 below, enveloped by two jackets. Within each T-junction there was a designed volume of 8.56 μ L. On the top in Figure 1, the 16 T-junctions are connected to a 17-mL bi-furcating flow distributor (FD). The COSMIC device was 3D-printed in a titanium alloy (Ti-6Al-4V), using a selective laser melting (SLM) printer.

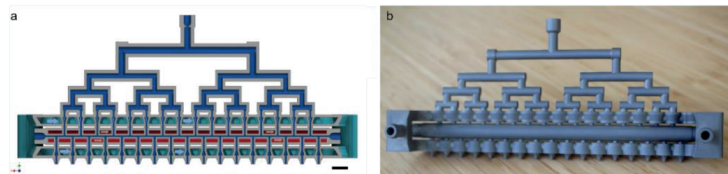


Figure 1. a) CAD image and b) photograph of the COSMIC device, which was 3D-printed in titanium alloy (Ti-6Al-4V).

The TWIST device (Figure 2) consists of two parts, viz. an internal and an external one. The ¹D separation takes place in the channel of the internal part. The external part consists of a bifurcating FD, a casing for the internal channel, and a series of the parallel ²D channels. The 3D-printed version of the TWIST slightly differs from the original design reported before⁶. The internal channel is 100 mm long and has an ID of 1 mm. In the present work it was attempted to achieve complete sealing between the internal part and a stainless-steel rod, which replaced the external part for this experiment. A Teflon sleeve was inserted as a seal between the internal and part and the rod, which had 17 through-holes drilled through the top and bottom.



Figure 2. a) top view and b) axial view of the 3D-printed metal version of the internal part of the TWIST with through holes (titanium alloy, Ti-6Al-4V; appearing dark coloured) and the stainless-steel metal rod with Teflon sleeve and through holes (external part) used in some of the experiments described in this paper.

The computer-aided-design (CAD) files of the COSMIC-2D and SLIT devices were created using Autodesk Inventor 2018 (San Rafael, CA, USA). The models were 3D-printed with a selective-laser-melting (SLM) system, using the aforementioned Ti alloy. 10-32 HPLC threads were then tapped into the fitting slots of the three pieces.

5.2.3 Experimental setups

The previously described COSMIC device and the improved version developed in the present work were used in a set-up is similar to that described by Passamonti *et al.*⁹ The temperatures of the heating and cooling jackets were adjusted based on the purpose. For the polymerization of a poly(styrene-co-divinylbenzene) or PS-DVB monolith, the heating and cooling jackets were set at 70°C and 4°C, respectively. For the polymerization of the poly(acrylamide-co-N,N'-methylenebisacrylamide) or poly(AA-co-MbA) monolith, the heating and cooling jackets were set at 60°C and 4°C, respectively. To confine the ¹D separation using the FTV approach, the temperatures used were 3°C and -5°C in the heating and cooling jackets, respectively.

5.2.4 In-situ synthesis of monolithic stationary phases

After 3D-printing, the titanium devices were sonicated and flushed with water and dried with compressed air several times to remove debris from the fabrication. The devices were then put in a furnace (AAF 1100, Carbolite Gero, Neuhausen, Germany) and heated at 5°C/min. Once the furnace reached 500°C, it was kept at this temperature for 6 h and then brought back to room temperature with a ramp of 10°C/min.

Titanium devices and glass-lined tubing were etched and then silanized for 90 min by flushing through a 20% (v/v) γ -MAPS solution in Tol at 10 $\mu\text{L}/\text{min}$. Thereafter, the surface-modified devices and capillaries were flushed with Tol and dried with nitrogen.

Small PS-DVB monoliths were created within each of the 33 slots of the 3D-printed COSMIC device. An alumina (Al_2O_3) bed was used to purify the monomer and the crosslinker. To achieve this, a polymerization mixture consisting of 20% STY, 20% DVB, 52% 1-decanol, 8% THF (all by weight) was prepared and used to fill the COSMIC completely. Thermal free-radical polymerization was initiated in the 33 designated regions using 2% AIBN with respect to the monomers, as described by Passamonti *et al.*¹⁰ The polymerization was performed at 70°C for 24 h. The same polymerization mixture was also used to create a PS-DVB monolith inside the SLIT. The polymerization mixture used to create the poly(AA-co-MbA) monolith consisted of 12.5% AA, 12.5% MbA, 21.5% OctOH, 40.1%, 13.4% and 1% (with respect to the monomers) AIBN (all by weight). The polymerization took place at 60°C for 24 h. After polymerization, the devices and tubings were thoroughly flushed with ACN.

5.2.3 Preparation of packed columns and devices

The COSMIC and the SS tubing were packed by preparing a slurry of 0.1 g/mL of 30 to 40 μm C18 particles with 120 Å pores (Chromatorex, Aichi-ken, Japan) in a 50:50 (by volume) mixture of purified water and IPA. The slurry was inserted in an empty column (150 mm \times 7 mm), which was then connected to the SS tubing. The latter was equipped with a SS union and frit (VICI) at the opposite extremity. In case of the COSMIC device, as short (about 50 mm) PEEK tubing was needed to connect it to the packing column. Similarly, a short capillary connected the exit of the COSMIC device to a frit. A flow of 1 mL/min of the packing solvent was used and this flow rate was maintained for 30 min after the packing was complete.

5.2.4 LC characterization

All chromatographic experiments were performed on a Waters Acquity UPLC system (Waters, Milford, MA, USA), equipped with a binary solvent manager, a temperature-controlled autosampler and a tunable dual-wavelength UV-Vis (TUV) detector.

Permeability and porosity. The permeability (K_f) of monoliths, prepared in the glass-lined tubing, SS tubing, and in the 3D-printed device, was evaluated using ACN at several flow rates. using Darcy's law¹¹

$$K_f = \frac{F_m \eta L}{\Delta P \pi r^2} \quad (5.1)$$

Where F_m is the flow rate of the solvent, η is its dynamic viscosity, ΔP is the pressure drop across a presumed cylindrical channel, L its length and r its radius.

An unretained compound (Ura for RP or Tol for HILIC) was used to determine the void volume (V_0) and the void time (t_0) of the channel.

Reversed-phase LC with UV detection. In the SS tubing and in the COSMIC device, the compounds were analysed using isocratic runs with of 85:15 water: ACN and 90:10 water: ACN, respectively (by volume). The samples were prepared in a solution of 80:20 water:ACN at a concentration of 0.1 mg/mL.

Hydrophilic-interaction LC with UV detection. Several compounds were analysed in the glass-lined tubing using a scouting gradient from 95% to 5% of ACN. The samples were prepared in a solution of 20:80 water: ACN at a concentration of 1 mg/mL.

Temperature effect. When the ¹D separation takes place in the COSMIC device, the temperature of the channel was around 3°C. To evaluate the effect of the temperature on the separation, we injected phenol on a packed SS tubing at room temperature and at 3°C (tubing submerged in the water bath).

5.3 Result and discussions

5.3.1 Development of devices: COSMIC-2D and SLIT

A two-dimensional COSMIC (COSMIC-2D) device was designed with a heating jacket enveloping a horizontal target channel of 1 mm ID and 100 mm length. This channel contains 8 T-junctions (FTVs) connected to a 0.647 mL bi-furcating flow-distributor (top) and 9 towards ²D channels (bottom), enveloped by two cooling jackets. Each T-junction has an internal volume of 9.42 μ L.

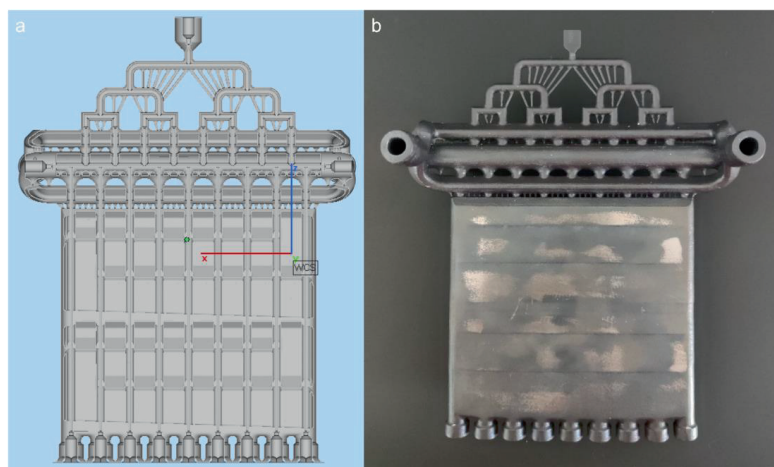


Figure 3. Complete COSMIC-2D device a) CAD image, b) photograph of device 3D-printed in titanium alloy Ti-6Al-4V.

The SLIT consists of three parts, *viz.* a movable rectangular part that contains a 1 mm ID channel with flow-through holes at the top and at the bottom, a FD part with 0.3 mL volume and a ²D separation part with 15 channels of 1 mm ID and 70 mm length. In the closed-position the movable part is compressed between two metal blades and the flow is confined within the channel. In the open-position the same part is aligned with the exit ports of FD and with the ²D channels to allow flushing from the FD inlet.

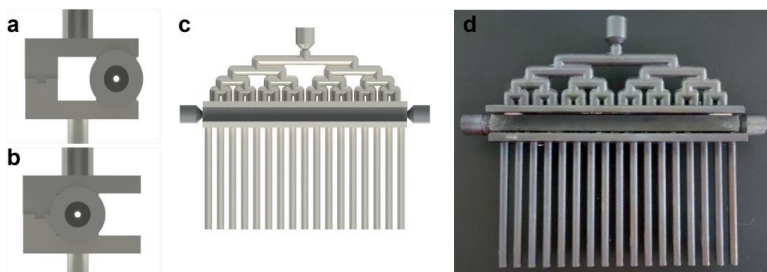


Figure 4. CAD image of the a) closed- and b) open-position of the SLIT device, c) CAD image of the SLIT device, d) photograph of the 3D-printed SLIT device in titanium alloy Ti-6Al-4V. For a close-up of the internal part see Figure 5.

5.3.2 *In-situ* creation of monolithic frits

PS-DVB monolithic stationary phases (frits) were created in the T-junction slots in the COSMIC and COSMIC-2D devices. The devices were filled completely with the polymerization mixture. The approach used to confine the polymerization is similar to the one described by Passamonti *et al.*⁹ The jacket around the ¹D separation channel of the device was kept at 10°C, while the jacket around the FTVs was set at 70°C. After 24 h, the device was flushed thoroughly with ACN. To confirm the formation of the monolithic frits, the device was then flushed from the FD inlet, while the ends of the ¹D separation channel were closed with blind nuts. The backpressure was recorded before and after the monolith formation. The backpressure before the monolith formation was negligible for both types of devices. After polymerization, the COSMIC and COSMIC-2D devices gave backpressures of 10 bar (with ACN) and 30 bar (with water), respectively, when flushed at 1 mL/min.

5.3.3 Achieving flow confinement

To help confine the flow in the COSMIC device, Wouters *et al.*⁵ suggested to create physical barriers. In the present study we attempted to create monolithic frits. Depending on the porosity of these, some spillage to the ²D separation channels may still take place. In contrast, the FTV approach allows the creation of frozen plugs inside the 33 T-junctions, which could confine the flow completely. From the CFD simulations, we concluded that a temperature of -4°C would suffice to create the aforementioned plugs. Unfortunately, simply setting the water bath at -4°C did not result in the formation of proper plugs, due to heat dissipation. Setting the temperature too low may result in the creation of a frozen layer also within the ¹D channel, obstructing the flow during separation or packing. After careful optimization, we found that temperatures of -12°C and 3°C in the cooling and heating jackets, respectively, led to good results with the COSMIC device. With these temperatures stable frozen plugs were created and the flow was fully confined within in the ¹D channel.

In the COSMIC-2D, the FTV approach was also attempted. The temperature of the (“heating”) jacket around the ¹D channel was varied from 1 to 35°C, while the temperature of the (cooling) jacket around the T-junctions was varied from -2 to -14°C. All combinations of temperatures resulted in either leakage into the ²D separation channels or formation of a frozen layer within the ¹D channel.

Confinement may also possibly be achieved by creating different permeabilities in the ¹D channel and in the ²D separation channels⁸. Since the COSMIC packed with the C18 particles gave a permeability

value of $K_{r,COSMIC} = 2.78 \times 10^{-11} \text{ m}^2$, which is at least two order of magnitude lower than that of poly(AA-co-MbA) monoliths¹², we proceeded with the creation of monoliths in the ²D separation channels. During this experiment, we discovered a leakage from some ²D channels into the surrounding jacket. This manufacturing defect rendered further experiments with the COSMIC-2D useless.

The internal part of the TWIST was polished, so as to reduce deviations from the CAD design to within 1%. Nevertheless, when the internal part and the SS rod with the Teflon sleeve inside (Figure 2) were assembled vast leakage occurred. The TWIST could not be used for further experiments and the SLIT arrangement was developed.

The SLIT design allows O-rings to be incorporated around the 33 holes of the ¹D separation channel. These O-rings are needed to provide additional sealing. Ethylene-Propylene-Diene-Monomer (EPDM) O-rings (2 mm ID, 1 mm thickness) were inserted in slots around each of the holes, as demonstrated in Figure 5.



Figure 5. 3D-printed internal part of the SLIT device with O-rings and a monolith created *in-situ*. Indicated scale is in cm.

In the closed-position (holes not aligned with the external part), the SLIT was flushed firstly with water and then with ACN, varying the flow rate from 1 to 50 $\mu\text{L}/\text{min}$. While no leakage was found when flushing with water, the SLIT showed some leakage when with flushing with ACN at flow rate exceeding 10 $\mu\text{L}/\text{min}$. After the EPDM O-rings were replaced with perfluoroelastomer (FFKM) O-rings, which are known to exhibit better solvent resistance, the experiments with ACN were repeated and no leakage was observed.

5.3.4 Packing of channels in COSMIC devices

To pack the ¹D channel in a COSMIC device or to perform a ¹D separation, a flow needs to be confine within the ¹D separation channel. Flow confinement was achieved by creating frozen plugs inside the 33 T-junctions.

The presence of the frozen plugs restricts the range of solvents that can be used to perform chromatographic separations. To test the resistance of the frozen plugs to organic solvents, we flushed the channel with increasing percentages of ACN for 30 min at each composition. At high percentages of ACN, the frozen plugs melted, and the flow confinement was lost. At up to 15% of ACN in water, we could flush the ¹D separation channel for more than 30 min.

Obviously, this severely limits the possibilities for chromatographic separations and the selection of packing solvents. Several mixtures of water and ACN in different ratios were investigated as packing solvents. A high percentage of ACN would cause the frozen plugs to melt, while a low percentage would cause the particles aggregate and precipitate. Finally, compromise conditions were established, which

consisted of a 50:50 IPA:water mixture to prepare the slurry and a 15:85 ACN:water mixture to replace the slurry solvent.

COSMIC devices and SS tubing were packed using a flow rate of 1 mL/min, until the backpressure stabilized (typically at about 220 or 140 bar, respectively).

5.3.5 Toward spatial-LC: offline temporal-RP×HILIC in capillary

The feasibility of our approach was first tested in capillaries. Specifically, packed SS tubing was used to perform the RP separations of a sample containing uracil, thiourea, benzamide, phenol, benzyl alcohol, acetophenone, benzonitrile and pyridine. In contrast, the HILIC separation was performed using the glass-lined tubing, in which we created a poly(AA-co-MbA) monolith.

Nawada [HPLC 2019, Milano] has shown that in some cases isocratic experiments may be preferred to gradient-elution experiments in spatial LC. In the present isocratic separation was attempted.

Figure 6 shows an overlay of the elution profiles of the individual analytes. Thiourea and uracil co-elute around t_0 , as do acetophenone, benzonitrile and benzyl alcohol. The pyridine peak has a significant tail, which overlaps with the phenol peak. While the unretained compounds gave sharp peaks, the retained compounds gave broader peaks. This is largely due to the rate at which the peak emerges from the column. The peak width is proportional to $1+k$, where k is the retention factor of the analyte. Inside the column the peak width mainly depends on the distance travelled. If we stop the development just before the unretained peaks emerge from the column, these are broadest, while the late-eluting peaks remain as narrow bands close to inlet¹³. This implies that in an ultimate, ideal cosmic device the 2D channels may not be equally spaced.

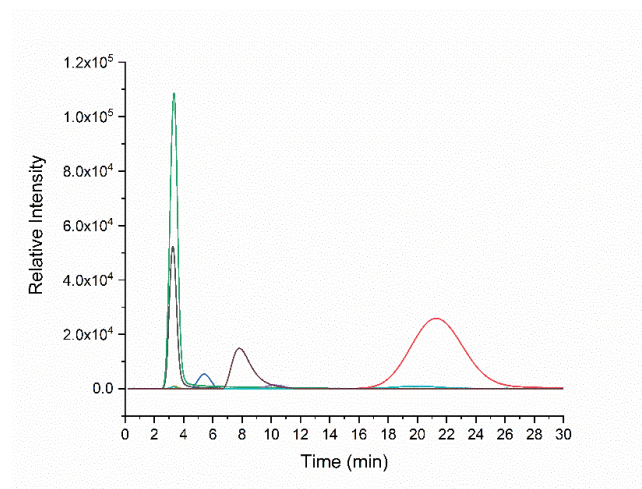


Figure 6. Individual injections of thiourea (black), acetophenone (red), benzamide (blue), uracil (green), phenol (purple), benzyl alcohol (yellow), benzonitrile (light blue) and pyridine (brown) in the packed tainless-steel tubing using an isocratic method. Mobile phase, 15:85 ACN:water (v/v). Analyses were carried out at room temperature, using a flow rate of 30 μ L/min and UV detection at 254 nm.

The retention factor of each analyte can be used to predict from which outlet of the COSMIC the compound will emerge. The results are shown in Table 1. It can be seen that the present mixture may

feasibly be spread across different channels in a spatial LC \square LC separation using a COSMIC or SLIT device.

Table 1. Retention times (t_R) and retention factors (k) obtained on a stainless-steel capillary and predicted outlet of the COSMIC for each analysed compound.

Compound	t_R (min)	k	Outlet
Thiourea	3.27	0	17
Uracil	3.27	0	17
Acetophenone	21.2	6	3
Benzamide	5.39	0.65	10
Benzyl alcohol	3.37	0.03	16
Benzonitrile	19.8	5.06	3
Phenol	10.3	2.15	5
Pyridine	7.84	1.40	7

For the 2D separation, the HILIC retention mechanism is targeted to separate the compounds that overlap within the 1D channel. A scouting gradient from 95 to 5% of ACN was applied to the compounds to demonstrate the feasibility of the approach.

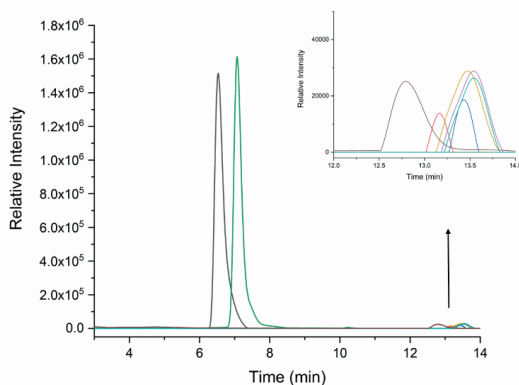


Figure 7. Individual injections of thiourea (black), acetophenone (red), benzamide (blue), uracil (green), phenol (purple), benzyl alcohol (yellow), benzonitrile (light blue) and pyridine (brown) in the poly(AA-co-MbA) monolithic column using a gradient from 95 to 5% of ACN in 30 min. Analyses were carried out at room temperature, using a flow rate of 30 μ L/min and UV detection at 254 nm. The insert shows an enlargement of the peaks eluting between 12 and 14 min. The truncated peaks are an artefact of the UV detector used.

Uracil and thiourea are partially separated, as are acetophenone, benzyl alcohol and benzonitrile. Pyridine and phenol are fully resolved. A further optimization of the gradient (e.g., from 95 to 60% B) may improve the separating our compounds, but no further optimization was done, since the COSMIC-2D was not usable. To successfully implement a spatial RPLC \square HILIC separation, one should also address breakthrough, caused by the high amounts of water transferred from the 1D channel to the 2D channels. Some kind of active modulation¹⁴ will eventually be needed.

5.3.6 Temporal 1D-LC in the COSMIC device

After testing the offline methods, the RP separations were carried out also in the COSMIC device. Some separation could be obtained, but the observed peaks – although approximately Gaussian – were very broad, especially for acetophenone and benzyl alcohol. In Table 2 the retention times, retention factors and peak widths (at the base) of the analysed compounds are reported. The retention times and, consequently, the retention factors of the compounds differ substantially to the ones found when carrying out the separations in the SS tubing. In principle, differences in retention times may be caused by small differences in the dimensions and volume of the COSMIC device and the SS tubing (134 μL vs 157 μL), but retention factors should not be affected. Differences in retention factors may be due to differences in the temperature at which the RP separations were carried out. While the analyses in the SS tubing were carried at room temperature, the jacket around the ^1D channel of the COSMIC device was kept at 3°C. Differences in the packing procedure and the density and homogeneity of the bed obtained will affect the retention times and, especially, the peak widths. Small differences in the observed retention factors may be found if the stationary phase is altered during the packing procedure or if the average particle size in the two channels differs, for example due to inhomogeneity of the slurry used for packing.

Table 2. Retention times (t_R), retention factors (k) and full widths of the peaks (w) of the compounds analysed in the ^1D channel of the COSMIC device.

Compound	t_R (min)	k	w (min)
Uracil	3.47	0	5
Acetophenone	39.4	10.3	32
Benzamide	8.04	1.3	4.5
Benzyl Alcohol	26.5	6.6	>35
Benzonitrile	33.6	8.7	14
Phenol	15.5	3.5	5

To assess the influence of the temperature, an individual injection of phenol was carried out keeping the SS tubing submerged in a water bath kept at 3°C. The retention time was found to increase from 10.3 to about 14.3 min and a broader peak shape was noticed. The retention factor changed from 2.15 to 2.9, closer to the value of 3.47 obtained on the COSMIC device. For other compounds the differences between the SS column (at room temperature) and the COSMIC device (at 3°C) are much greater than for phenol. The shift in retention factor of benzyl alcohol (from 0.03 to 6.6) is the most remarkable. Several explanations are possible. The temperature may not be uniform across the ^1D channel in the COSMIC device. The COSMIC device was insulated and its external temperature was kept constant during the whole analysis, but the mobile phase was not cooled before entering the device¹⁵. A second explanation may be limited miscibility of water and ACN at low temperatures¹⁶. Finally, the inner surface of the channel consisted of titanium oxide. Oxidation of the titanium surface is necessary to create a monolithic stationary phase in the channel that is attached to the wall. However, when the channel is packed the active titanium surface may create a secondary retention mechanism with a limited capacity.

The non-polar RP surface and the polar TiO₂ surface together create a very heterogenous system. The intra-day variation of the retention times was within 5%, but the inter-day variation reached 20%.

5.4 Conclusions

The COSMIC-2D device and the SLIT device were designed and 3D-printed successfully. While the former, due to a manufacturing defect, could not be tested fully, the latter showed significant potential. We successfully confined the flow in the ¹D channel of the COSMIC and SLIT devices. In the COSMIC device the flow confinement was achieved using integrated freeze-thaw valves (FTV), which created frozen plugs in and around the inlets of the ¹D channel from the flow distributor (FD) and the outlets towards the second-dimension (²D) channels. In the SLIT device, the flow was confined by misaligning the openings in the first-dimension (¹D) channel with the outlets of the FD and the inlets of the ²D channels. The SLIT approach is based on the presence of a physical barrier. The sealing was improved by inserting O-rings. We successfully demonstrated the feasibility of an RPLC×HILIC separation of a mixture of small compounds by offline experiments in capillaries and we successfully transfer the temporal-RP separation to the COSMIC device.

Several challenges need to be addressed to make this technology and approach successful. The limited number of ²D channels greatly limits the attainable peak capacity and cause much dilution when transferring fractions from the ¹D separation. In the present design, flushing caused each fraction to be diluted 2000 times. To inspect the different fractions and confirm the presence of the different analytes in the predicted outlets some sort of enrichment (active modulation) is required at the top of the 2D channels, a process that was not tested so far. In case of RPLC×HILIC separations active modulation to avoid dilution and breakthrough is not straightforward. In the COSMIC device the FTV approach made it necessary to perform ¹D separations at low temperatures (3°C). The SLIT approach allows operation at ambient (or higher) temperatures, which is generally more favourable. The COSMIC device was developed with the intention to create monolithic stationary phases, which is why the inner surface was oxidized to obtain a titanium-oxide (TiO₂) layer. This is highly unfavourable when the ¹D channel is packed with reversed-phase particles. Silanization of the surface may help to some extent. A more-homogeneous ¹D separation channel may also be obtained by packing an oxidized titanium channel with TiO₂ particles for performing NPLC or HILIC separations.

References

- (1) Beck, M.; Claassen, M.; Aebersold, R. Comprehensive Proteomics. *Curr. Opin. Biotechnol.* **2011**, *22* (1), 3–8. <https://doi.org/10.1016/J.COPBIO.2010.09.002>.
- (2) Pirok, B. W. J.; Gargano, A. F. G.; Schoenmakers, P. J. Optimizing Separations in Online Comprehensive Two-Dimensional Liquid Chromatography. *J. Sep. Sci.* **2018**, *41* (1), 68–98. <https://doi.org/10.1002/JSSC.201700863>.
- (3) Wouters, B.; Davydova, E.; Wouters, S.; Vivo-Truyols, G.; Schoenmakers, P. J.; Eeltink, S. Towards Ultra-High Peak Capacities and Peak-Production Rates Using Spatial Three-Dimensional Liquid Chromatography. *Lab Chip* **2015**, *15* (23), 4415–4422. <https://doi.org/10.1039/C5LC01169H>.
- (4) Liu, J.; Chen, C.-F.; Yang, S.; Chang, C.-C.; Devoe, D. L. Mixed-Mode Electrokinetic and Chromatographic Peptide Separations in a Microvalve-Integrated Polymer Chip †. <https://doi.org/10.1039/c003505j>.
- (5) Wouters, B.; De Vos, J.; Desmet, G.; Terry, H.; Schoenmakers, P. J.; Eeltink, S. Design of a Microfluidic Device for Comprehensive Spatial Two-Dimensional Liquid Chromatography. *J. Sep. Sci.* **2015**, *38* (7), 1123–1129. <https://doi.org/10.1002/jssc.201401192>.
- (6) Adamopoulou, T.; Deridder, S.; Desmet, G.; Schoenmakers, P. J. Two-Dimensional Insertable Separation Tool (TWIST) for Flow Confinement in Spatial Separations. *J. Chromatogr. A* **2018**, *1577*, 120–123. <https://doi.org/10.1016/J.CHROMA.2018.09.054>.
- (7) Nawada, S. H.; Aalbers, T.; Schoenmakers, P. J. Freeze-Thaw Valves as a Flow Control Mechanism in Spatially Complex 3D-Printed Fluidic Devices. *Chem. Eng. Sci.* **2019**, *207*, 1040–1048. <https://doi.org/10.1016/j.ces.2019.07.036>.
- (8) Adamopoulou, T.; Deridder, S.; Bos, T. S.; Nawada, S.; Desmet, G.; Schoenmakers, P. J. Optimizing Design and Employing Permeability Differences to Achieve Flow Confinement in Devices for Spatial Multidimensional Liquid Chromatography. *J. Chromatogr. A* **2020**, *1612*, 460665. <https://doi.org/10.1016/J.CHROMA.2019.460665>.
- (9) Passamonti, M.; Bremer, I.; Nawada, S. H.; Currivan, S.; Gargano, A.; Schoenmakers, P. Confinement of Monolithic Stationary Phases in Targeted Regions of 3D-Printed Titanium Devices Using Thermal Polymerization. *Anal. Chem.* *92* (3), 2589–2596. <https://doi.org/10.1021/acs.analchem.9b04298>.
- (10) Chen, H.; Fan, Z. H. Two-Dimensional Protein Separation in Microfluidic Devices. *Electrophoresis* **2009**, *30* (5), 758–765. <https://doi.org/10.1002/elps.200800566>.
- (11) Les Fontaines Publiques de La Ville de Dijon : Exposition et Application Des Principes à Suivre et Des Formules À [...].
- (12) Passamonti, M.; De Roos, C.; Schoenmakers, P. J.; Gargano, A. F. G. Poly(Acrylamide- Co- N, N'-Methylenabisacrylamide) Monoliths for High-Peak-Capacity Hydrophilic-Interaction Chromatography-High-Resolution Mass Spectrometry of Intact Proteins at Low Trifluoroacetic Acid Content. *Anal. Chem.* **2021**, *93*, 16000–16007. https://doi.org/10.1021/ACS.ANALCHEM.1C03473/SUPPL_FILE/AC1C03473_SI_001.PDF.
- (13) Giddings, J. C. Dynamics of Chromatography: Principles and Theory. *Dyn. Chromatogr. Princ. Theory* **2017**, 1–323. <https://doi.org/10.1201/9781315275871>.
- (14) Gargano, A. F. G.; Duffin, M.; Navarro, P.; Schoenmakers, P. J. Reducing Dilution and Analysis Time in Online Comprehensive Two-Dimensional Liquid Chromatography by Active Modulation. *Anal. Chem.* **2016**, *88* (3), 1785–1793. <https://doi.org/10.1021/ACS.ANALCHEM.5B04051>.
- (15) Welsch, T.; Schmid, M.; Kutter, J.; Kálmán, A. Temperature of the Eluent: A Neglected Tool in High-Performance Liquid Chromatography? *J. Chromatogr. A* **1996**, *728* (1–2), 299–306. [https://doi.org/10.1016/0021-9673\(95\)00876-4](https://doi.org/10.1016/0021-9673(95)00876-4).
- (16) Shao, G.; Agar, J.; Giese, R. W. Cold-Induced Aqueous Acetonitrile Phase Separation: A Salt-Free way to Begin QuEChERS. *J. Chromatogr. A* **2017**, *1506*, 128. <https://doi.org/10.1016/J.CHROMA.2017.05.045>.